

ORIGINAL  
RESEARCH

R. Della Nave  
A. Ginestroni  
C. Tessa  
M. Giannelli  
S. Piacentini  
M. Filippi  
M. Mascalchi



# Regional Distribution and Clinical Correlates of White Matter Structural Damage in Huntington Disease: A Tract-Based Spatial Statistics Study

**BACKGROUND AND PURPOSE:** HD entails damage of the WM. Our aim was to explore in vivo the regional volume and microstructure of the brain WM in HD and to correlate such findings with clinical status of the patients.

**MATERIALS AND METHODS:** Fifteen HD gene carriers in different clinical stages of the disease and 15 healthy controls were studied with T1-weighted images for VBM and DTI for TBSS. Maps of FA, MD, and  $\lambda_{\parallel}$  and  $\lambda_{\perp}$  were reconstructed.

**RESULTS:** Compared with controls, in addition to neostriatum and cortical GM volume loss, individuals with HD showed volume loss in the genu of the internal capsule and subcortical frontal WM bilaterally, the right splenium of the corpus callosum, and the left corona radiata. TBSS revealed symmetrically decreased FA in the corpus callosum, fornix, external/extreme capsule, inferior fronto-occipital fasciculus, and inferior longitudinal fasciculus. Areas of increased MD were more extensive and included arciform fibers of the cerebral hemispheres and cerebral peduncles. Increase of the  $\lambda_{\parallel}$  and a comparatively more pronounced increase of the  $\lambda_{\perp}$  underlay the decreased FA of the WM in HD. Areas of WM atrophy, decreased FA, and increased MD correlated with the severity of the motor and cognitive dysfunction, whereas only the areas with increased MD correlated with disease duration.

**CONCLUSIONS:** Microstructural damage accompanies volume decrease of the WM in HD and is correlated with the clinical deficits and disease duration. MR imaging-based measures could be considered as a biomarker of neurodegeneration in HD gene carriers.

**ABBREVIATIONS:** corr = corrected; DTI = diffusion tensor imaging; FA = fractional anisotropy; FDR = false discovery rate; FMRIB = Oxford Centre for Functional MRI of the Brain; FSL = FMRIB Software Library; GM = gray matter; HD = Huntington disease; L = left;  $\lambda_{\parallel}$  = axial diffusivity;  $\lambda_{\perp}$  = radial diffusivity; MD = mean diffusivity; SPM = Statistical Parametric Mapping; TBSS = Tract-Based Spatial Statistics; UHDRS = Unified Huntington's Disease Rating Scale; VBM = voxel-based morphometry; WM = white matter; R = right

HD is an autosomically dominant inherited condition due to expansion of a CAG triplet in a gene on chromosome 4 encoding a protein named huntingtin.<sup>1</sup> Neuropathologic examination indicated that HD is primarily a disease of the GM, leading to atrophy of the striatum and the cerebral cortex and that WM degeneration becomes evident in a more advanced phase of the disease.<sup>2</sup> However, MR imaging studies demonstrated that atrophy of the cerebral WM is already detectable in presymptomatic or early symptomatic HD carriers<sup>3-6</sup> and is variably advanced in symptomatic HD.<sup>7-9</sup>

Moreover several diffusion-weighted imaging and DTI studies revealed microstructural damage of the residual WM in HD.<sup>10-14</sup> A role for WM damage has been proposed in ex-

plaining the varying and complex symptoms of this condition.<sup>11-13</sup>

Recently, a voxelwise automatic whole-brain method for the investigation of WM microstructure based on multisubject diffusion tensor data without any bias due to an a priori knowledge, called TBSS, was developed.<sup>15,16</sup> TBSS has been applied to the investigation of a few inherited ataxias<sup>17,18</sup> and was preliminarily used to investigate the progression of WM damage in pre- and early-symptomatic HD carriers.<sup>14</sup>

We assessed, with VBM, the regional WM volume and, with TBSS, the distribution of the brain WM microstructural damage in patients with HD and correlated these findings with the number of triplets, disease duration, and severity of the motor and cognitive dysfunction.

## Materials and Methods


Twenty carriers of the HD gene (8 women, 12 men; mean age,  $56 \pm 13$  years) consecutively observed at the Outpatient Clinic for Movement Disorders of the University of Florence, Florence, Italy, participated in this prospective study, which was approved by the local ethics committee. Molecular diagnosis was made according to a previously reported method,<sup>19</sup> and the triplet number in the HD carriers ranged between 39 and 50 (normal value,  $\leq 32$ ).<sup>20</sup> Images of 5 HD carriers showed motion artifacts and were excluded from analyses. The genetic and clinical characteristics of the 15 (7 women and 8 men) successfully imaged HD carriers are detailed in Table 1.


Fifteen age-matched healthy volunteers (7 women, 8 men; mean

Received February 15, 2010; accepted after revision March 16.

From the Radiodiagnostic Unit (R.D.N.), San Giuseppe Hospital, Empoli, Italy; Radiodiagnostic Section (A.G., M.M.), Department of Clinical Physiopathology, and Department of Neurological and Psychiatric Sciences (S.P.), University of Florence, Florence, Italy; Radiology Unit (C.T.), Versilia Hospital, Camaiore (Lucca), Italy; Department of Medical Physics (M.G.), Pisa Hospital, Pisa, Italy; and Neuroimaging Research Unit (M.F.), Department of Neurology, Scientific Institute and University San Raffaele, Milan, Italy.

Please address correspondence to Mario Mascalchi, PhD, Radiodiagnostic Section, Department of Clinical Physiopathology, University of Florence, Viale Morgagni 85, 50134, Florence, Italy; e-mail: m.mascalchi@dfc.unifi.it

 indicates article with supplementary on-line tables.

 indicates article with supplementary on-line figures.

DOI 10.3174/ajnr.A2128

**Table 1: Genetic and clinical features in 15 HD gene carriers**

	Mean	Range
Age (yr)	56 ± 12	34–75
CAG repeat size	44 ± 3	40–50
Sex (M/F)	8/7	
Disease duration (years)	6.9 ± 6.6	0–28
UHDRS motor score	33 ± 18	0–57
Verbal Fluency test	13 ± 11	3–40
Symbol Digit test	19 ± 19	0–66
Stroop Color-Word Interference test	25 ± 34	3–120

age, 55 ± 12 years) unrelated to the HD carriers and without a family history of neurologic diseases served as controls. HD gene carriers and controls provided written informed consent before entering the study.

At the time of the MR imaging examination, the same neurologist defined disease duration in the HD gene carriers and computed the score on the UHDRS.<sup>21</sup> This includes evaluation of motor symptoms and 3 selected timed tests,<sup>22</sup> namely Verbal Fluency, Stroop Color-Word Interference<sup>23</sup> and Symbol Digit tests,<sup>24</sup> which are sensitive to frontal-striatal dysfunction in HD<sup>21</sup> and showed correlation with cerebral WM volume.<sup>4,7</sup>

The clinical stages as determined by their total functional capacity score were also determined by using the criteria defined by Shoulson and Fahn.<sup>25</sup> These 5 stages take into account an individual's engagement in an occupation; the ability to handle financial affairs, manage domestic responsibilities, and perform activities of daily living; and his or her need for care facilities. One of the gene carriers was pre-symptomatic (stage I); 4 had very mild impairment (stage II); 6, mild impairment (stage III); and 4, moderate impairment (stage IV).

Eleven HD carriers were in continuous treatment with serotonin reuptake inhibitors, tricyclic antidepressants, or haloperidol.

### MR Imaging Examination

Patients and controls underwent MR imaging on a 1.5T system (Intera; Philips Healthcare, Best, the Netherlands) with a 33 mT/m maximum gradient strength and sensitivity encoding coil technology. After scout and axial proton density and T2-weighted images (TR = 2242 ms, TE = 20/90 ms, FOV = 256 mm, matrix size = 256 × 288, 20 sections, section thickness = 5 mm, NEX = 2), axial DTI with a single-shot echo-planar imaging sequence (TR = 9394 ms, TE = 89 ms, FOV = 256 mm, matrix size = 128 × 128, 50 sections, section thickness = 3 mm, no gap, NEX = 3) was also obtained for the TBSS analysis. Diffusion-sensitizing gradients were applied along 15 non-collinear directions by using a b-value of 0 (B0 image) or 1000 s/mm<sup>2</sup>. After automatic segmentation of the brain from the nonbrain tissue and correction for head motion and distortions due to eddy currents by means of the FMRIB Diffusion Toolbox 2.0,<sup>26</sup> part of the FSL 4.0 (FMRIB Image Analysis Group, Oxford, United Kingdom),<sup>27</sup> maps of FA, MD, and of the greatest ( $\lambda_1$ ), middle ( $\lambda_2$ ) and smallest ( $\lambda_3$ ) individual eigenvalues of the diffusion tensor were calculated from DTI. From the individual eigenvalues of the diffusion tensor, we computed  $\lambda_{||}$  and  $\lambda_{\perp}$ , taking into account that  $\lambda_{||}$  is equal to  $\lambda_1$  and  $\lambda_{\perp}$  is equal to  $(\lambda_2 + \lambda_3) / 2$ .

To assess regional volume differences with VBM, we finally acquired a sagittal 3D T1-weighted turbo gradient-echo sequence (TR = 8.1 ms, TE = 3.7 ms, flip angle = 8°, inversion time = 764 ms, FOV = 256 mm, matrix size = 256 × 256, 160 contiguous sections, section thickness = 1 mm).

The acquisition time of the entire protocol was approximately 20 minutes.

### Data Processing

T1-weighted images, source DTIs, and DTI-derived maps were visually evaluated for motion artifacts before entering further image processing. Those without motion artifacts entered the analyses detailed below.

Image data processing was performed on a PC running the SPM2 software (Wellcome Department of Cognitive Neurology, London, United Kingdom) for VBM and the FSL 4.0 package for TBSS.

The methodology for optimized VBM closely followed that previously reported.<sup>28</sup> TBSS analysis was performed by using TBSS 1.1 tool, part of FSL 4.0, and is described in detail elsewhere.<sup>15,16</sup> Briefly, TBSS implies a 4-step approach: identification of a common registration target and alignment of all subjects' FA images to this target; creation of the mean of all aligned FA images and of a skeletonized mean FA image, which is thresholded; projection of each subject's FA image onto the skeleton; and voxelwise statistical analysis across subjects on the skeleton-space FA data. Using the same nonlinear registration, we projected the skeleton and skeleton projection vectors derived from the FA, MD,  $\lambda_{||}$ , and  $\lambda_{\perp}$  data onto the skeleton before voxelwise statistical analysis.<sup>16</sup>

### Statistical Methods

**VBM.** Statistical analysis of the MR imaging data was based on the general linear model and the theory of Gaussian random fields. A voxelwise comparison of spatially normalized T1-weighted images was made by using SPM2. Group comparisons were performed by means of analysis of covariance by using the total volume of each segmented image (GM volume for GM analysis, WM volume for WM analysis) as confounding covariates. Choice of the latter instead of intracranial volume was made to explore the areas that, in the context of a generalized brain atrophy, are those more specifically involved in HD. Age and sex were included as covariates of no interest to exclude possible effects of these variables on regional GM or WM volumes.<sup>28</sup> Voxel-level analysis with a significance threshold set at a *P* value of .05, corrected for multiple comparisons across the whole brain (FDR correction), was applied to the resulting *t*-statistic maps of GM and WM.

To correlate the amount of GM or WM volume loss with genetic and clinical variables in HD gene carriers, we performed parametric VBM analysis. Statistical analysis was based on linear regressions of the local GM or WM value in each voxel of the whole brain, without normalization to the total GM or WM volume, using the number of triplets, disease duration, and UHDRS scores. The hypotheses of a direct or inverse correlation between both volume and genetic and clinical variables were evaluated. A statistical threshold of *P* < .05 corrected (FDR correction) for multiple comparisons was applied.

**TBSS.** Group comparisons of FA, MD,  $\lambda_{||}$ , and  $\lambda_{\perp}$  data were performed by using a permutation-based nonparametric inference on cluster size<sup>29</sup> and Randomize 2.0 software, part of FSL 4.0. A restrictive statistical threshold was used (cluster-based thresholding, *t* > 3, *P* < .05, corrected for multiple comparisons).<sup>15</sup>

Identification of the abnormal WM tracts revealed by TBSS was based on the atlases made at Johns Hopkins University.<sup>30</sup>

In addition, in patients with HD, we correlated FA and MD values in each voxel of the whole brain with each HD carrier's number of triplets, disease duration, and UHDRS motor and cognitive scores by using the same software and permutation-based nonparametric inference on cluster size (*t* > 3, *P* < .05 corrected for multiple compar-

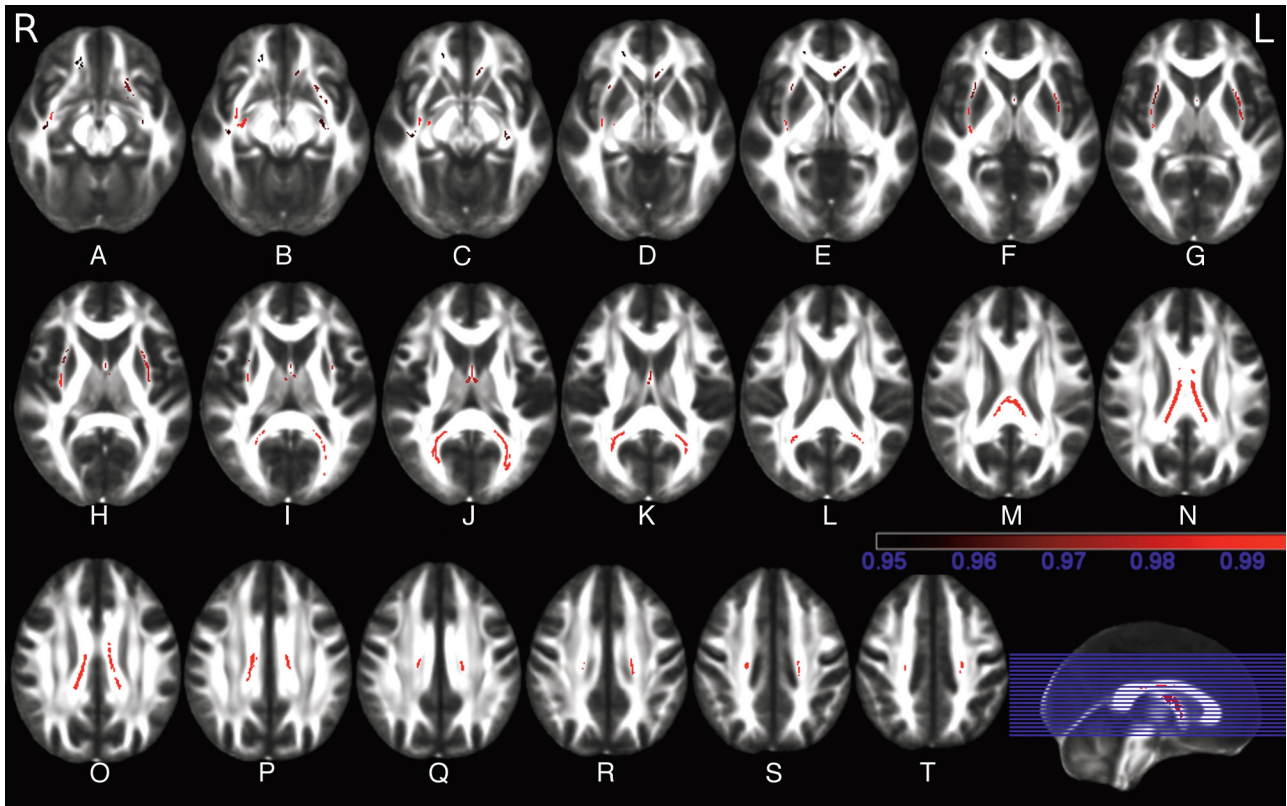


**Fig 1.** A–T, TBSS analysis of FA maps. Maps of the *t*-value ( $t > 3$  with  $P < .05$  corrected for multiple comparisons) show, in red, the areas of significantly reduced FA in WM tracts in HD gene carriers compared with controls. These include the corpus callosum and the external/extreme capsule bilaterally (color bar indicates *P* values).

**Table 2: TBSS results: areas of decreased or increased FA in 15 patients with HD versus 15 healthy controls**

FA	Cluster Size (mm <sup>3</sup> )	<i>P</i>	Coordinates (Local Maxima)			Areas
			X	Y	Z	
HD < controls	1447	.000	-10	-35	21	Body and splenium of corpus callosum, R and L corona radiata
	375	.005	-20	-49	9	L splenium of corpus callosum and forceps major
	317	.008	25	-53	10	R splenium of corpus callosum and forceps major
	302	.009	36	-8	14	R inferior fronto-occipital fasciculus
	201	.019	-34	-1	0	L external capsule
	181	.022	0	5	1	Fornix
	139	.032	30	14	-4	R external capsule
	136	.033	-21	15	-15	L inferior fronto-occipital and uncinata fasciculi
	129	.037	-9	24	-10	Genu of corpus callosum
	122	.040	-31	-10	-14	L inferior longitudinal fasciculus
	121	.041	41	-13	-17	R inferior longitudinal fasciculus
	106	.049	17	29	-16	R inferior fronto-occipital fasciculus
	HD > controls	405	.004	-26	-23	11
241		.011	24	22	5	R corticospinal tracts, anterior thalamic radiations, superior fronto-occipital fasciculus, and corona radiata

isons).<sup>15</sup> The hypotheses of a direct or inverse correlation between both FA and MD and genetic and clinical variables were evaluated.

## Results

Between-group VBM analysis showed symmetric GM volume losses in the caudate and putamen and multiple extensive cerebral cortical regions of the HD gene carriers compared with controls (On-line Fig 1 and On-line Table 1). WM volume difference was confined to the genu of the internal capsule and

subcortical frontal WM bilaterally, right splenium of the corpus callosum, and left corona radiata (On-line Fig 1 and On-line Table 1).

No clusters showing correlation between GM or WM volume change and number of triplets or disease duration were seen. Conversely clusters in the striatum and cerebral cortex showed significant ( $P < .05$ ) correlation between decreased GM volume and Motor Scale, Symbol Digit, Stroop Color-Word Interference, and Verbal Fluency tests (On-line Table

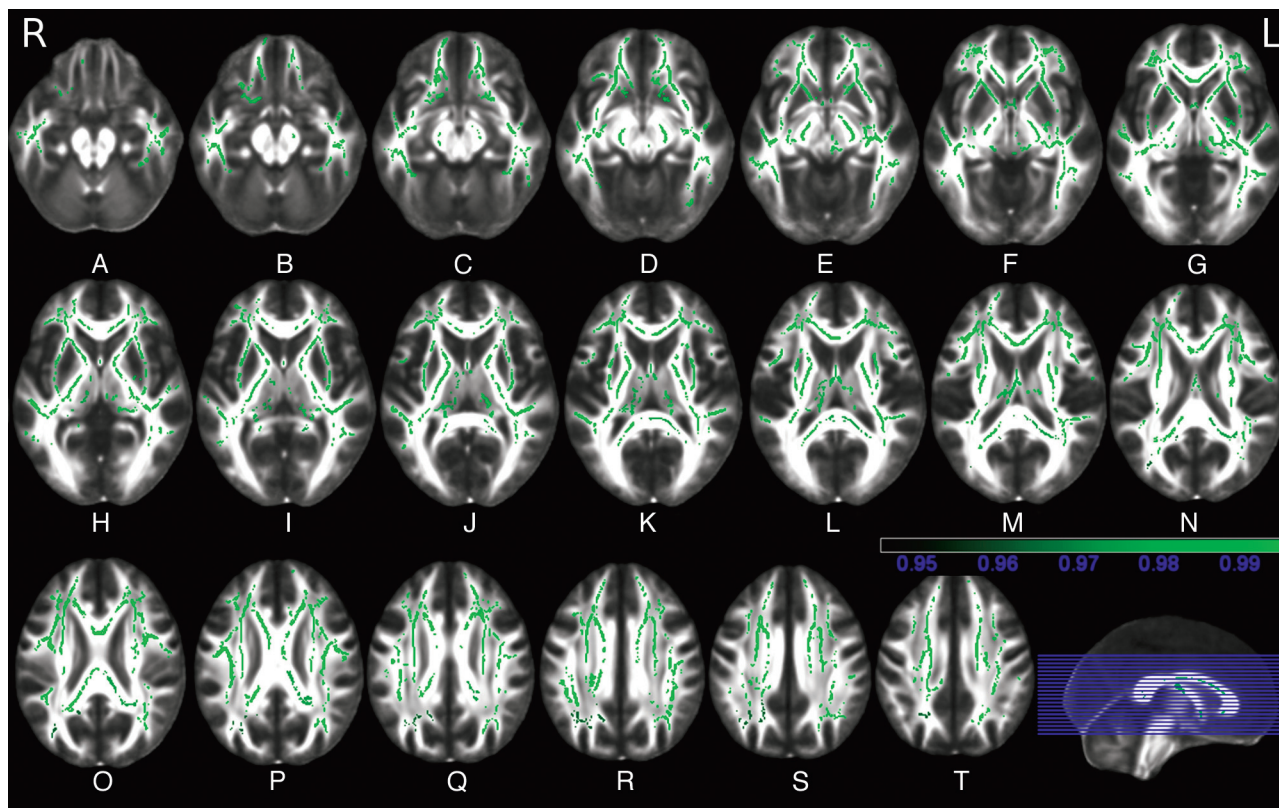


**Fig 2.** A–T, TBSS correlation results in HD gene carriers. Green shows the areas where MD correlates ( $t > 3$  with  $P < .05$  corrected for multiple comparisons) with the disease duration (color bar indicates  $P$  values).

2). Also extensive clusters in the frontal and temporal subcortical WM, genu of the corpus callosum, corticospinal tracts, middle and inferior cerebellar peduncles, and cerebellar WM showed correlation between decreased WM volume and Motor Scale and the scores of Symbol Digit, Stroop Color-Word Interference, and Verbal Fluency tests (On-line Table 2).

TBSS showed symmetrically decreased FA in the WM of the corpus callosum, fornix, external/extreme capsule, inferior fronto-occipital fasciculus, and inferior longitudinal fasciculus in HD carriers compared with controls (Fig 1 and Table 2). In these areas, analysis of the eigenvalues showed increased  $\lambda_{\parallel}$  and  $\lambda_{\perp}$  (On-line Fig 2).

Conversely, areas of increased FA were seen in the posterior limb of the left internal capsule, left superior longitudinal fasciculus, and, with a nearly symmetric distribution, in the supralenticular frontal WM comprising the corticospinal tracts, anterior thalamic radiations, superior fronto-occipital fasciculus, and corona radiata (On-line Fig 2 and Table 2). In these areas, the analysis of the eigenvalues showed increased  $\lambda_{\parallel}$ , whereas  $\lambda_{\perp}$  was unchanged (On-line Fig 2).

Areas of increased MD in HD carriers compared with controls were extensive and included, besides all the areas of increased or decreased FA, the arciform fibers of all the cerebral lobes, the corona radiata, and the corticospinal tracts in the right origin and left cerebral peduncle (On-line Fig 3 and On-line Table 3). The pons, medulla, and cerebellum WM were spared.

No area of decreased MD was detected in HD carriers.

Voxelwise correlations between the FA and MD data and clinical variables in HD gene carriers revealed several regions

in which variability in diffusion measurements correlated significantly with variability in function and, in the case of MD, also in disease duration.

Several clusters were observed in which decreased FA correlated with the motor score of the UHDRS (On-line Fig 4 and On-line Table 4) and with the Stroop Color-Word Interference (On-line Fig 5 and On-line Table 5) and Symbol Digit (On-line Fig 6 and On-line Table 6) scores. No correlation was observed for the number of triplets, Verbal Fluency, and disease duration. Most interesting, the clusters exhibiting correlation between decreased FA and the scores of the Stroop test were limited to the frontal WM (On-line Fig 5).

Analysis of the TBSS maps in the midsagittal plane revealed that the clusters of correlation between FA decrease and UHDRS were localized in the corpus callosum head, body, and splenium (with sparing of the genu), while those between FA decrease and Stroop and Symbol Digit were localized in the anterior (frontal) portion of the corpus callosum body, with additional clusters in the posterior portion of the body and in the head for the Symbol Digit test.

No clusters of significant correlation between increased FA and genetic or clinical features were observed.

Extensive clusters of correlation between increased MD and disease duration (Fig 2), motor score (On-line Fig 7), Verbal Fluency (On-line Fig 8), and Symbol Digit (On-line Fig 9) tests were observed throughout the cerebral hemispheres and the corpus callosum, with sparing of the brain stem and the cerebellum, while the areas of correlation with the Stroop Color-Word Interference test were limited to the antero-infer-

rior portion of the left frontal lobe, and no correlation was observed with the number of triplets.

## Discussion

The present investigation demonstrates that along with atrophy of the neostriatal and cerebral cortical GM, significant atrophy and microstructural damage of the cerebral WM are present in HD gene carriers and that the latter 2 correlate with clinical features, including disease duration and indexes of motor and cognitive impairment.

Neuropathology and MR imaging reveal selective GM atrophy in HD, with the earliest changes progressing from the dorsolateral to the ventromedial portions of the neostriatum.<sup>22</sup> In addition, the cerebral cortex is known to be affected selectively with an early involvement of the operculum.<sup>3,31</sup> Subsequently, progressive cortical thinning involves the primary sensory, motor, and visual cortices and then the primary auditory cortex and those cortical regions adjacent to the areas of early involvement.<sup>22</sup> Finally, atrophy extends to the entorhinal cortex and higher order cortical regions,<sup>22</sup> with a relative sparing of the limbic prefrontal cortex.<sup>32</sup> Regional atrophy of the cerebral WM in the periventricular and subinsular regions in the internal capsule and cerebellum was reported in previous volumetric MR imaging studies in presymptomatic and symptomatic HD carriers.<sup>3-9</sup> Hence the distribution of GM and WM atrophy reflecting irreversible tissue loss in our series of patients with HD is in line with prior reports.

Using diffusion-weighted imaging and region-of-interest analysis, we initially observed increased apparent diffusion coefficient in the neostriatum and cerebral periventricular WM in HD gene carriers.<sup>10</sup> The WM microstructural damage was confirmed by subsequent DTI studies in presymptomatic and early symptomatic HD carriers.<sup>11,12</sup> In particular, Reading et al<sup>11</sup> observed several clusters of decreased FA bilaterally in the cerebral WM in presymptomatic HD gene carriers. Rosas et al,<sup>12</sup> by using a combined region-of-interest and voxelwise approach, found decreased FA throughout the corpus callosum, in the posterior limb of the internal capsule, and in the frontal subcortical WM of presymptomatic individuals. In symptomatic HD gene carriers, the areas of decreased FA also included the external/extreme capsules; the WM in the vicinity of the sensorimotor cortex; frontal, parietal, and parieto-occipital areas; the cerebral peduncles; and the brain stem. Finally Klöppel et al<sup>13</sup> identified, in presymptomatic carriers of the HD gene, an increased FA in the putamen bilaterally and decreased FA in the anterior parts of the corpus callosum, as well as a reduction of frontal corticofugal streamlines arising from the frontal eye fields reaching the body of the caudate nucleus.

TBSS has 3 main advantages compared with other voxelwise analysis methods of DTI data.<sup>15</sup> First, TBSS overcomes the limitations caused by alignment inaccuracies and by uncertainty about smoothing extent, which are typical of other voxelwise methods of analysis of diffusion tensor data. Second, TBSS examines the main WM tracts exclusively, avoiding problems arising from misregistration shift of the gray/white boundary, which can occur in atrophic brains such as those of advanced HD.<sup>12,13</sup> Third, TBSS enables evaluation of the microstructure of specific WM tracts identified in the skeleton. In addition, the same skeletons can be used to assess changes in the FA and MD and of the eigenvalues of the diffusion tensor

reflecting  $\lambda_{\parallel}$  and  $\lambda_{\perp}$ . In particular, recent studies in murine models of WM diseases have indicated that analysis of  $\lambda_{\parallel}$  and  $\lambda_{\perp}$  might contribute more specific information about the physiopathologic processes responsible for the decreased FA and increased MD commonly observed in pathologic processes involving the WM.<sup>33</sup> In fact,  $\lambda_{\parallel}$  would be sensitive to axonal injury and degeneration, whereas  $\lambda_{\perp}$ , reflecting the degree of myelination, would be sensitive to demyelination.<sup>33</sup>

Using TBSS, Weaver et al<sup>14</sup> explored the progression of WM microstructural changes in 7 pre- or early-symptomatic HD carriers examined twice 1 year apart. They reported, between baseline and follow-up, a significant reduction of FA throughout the brain, including the corpus callosum, which better matched a decrease of  $\lambda_{\parallel}$ , consistent with axonal injury or withdrawal, rather than with an increase of  $\lambda_{\perp}$ , consistent with demyelination.

In the present study, we performed a regional assessment of the microstructure of the remaining brain WM in vivo by using TBSS. We examined a relatively small sample of HD carriers who, however, almost covered the entire range of clinical severity of the disease with the exception of the most severe one (stage V). This enabled us to preliminarily explore the capability of DTI to reflect the increasing severity of neurodegeneration. Furthermore, it permitted us to investigate the possible clinical significance of the WM changes.

We observed symmetrically decreased FA combined with increased MD in the WM of the external/extreme capsule and in the corpus callosum. Both features were previously reported.<sup>12,13</sup> In particular, the damage of the external capsule appears interesting because according to experimental observations,<sup>34</sup> the external capsule corresponds strictly to a corticostriatal fiber tract and its damage is expected because the putamen and the opercular cortex are among the major sites of GM neurodegeneration in HD. On the other hand, the substantial microstructural damage of the corpus callosum suggests that degeneration of the interhemispheric WM tracts connecting the degenerating cortical GM of the cerebral hemispheres is a key feature of the disease in its symptomatic clinical stages.

The pattern of decreased FA with corresponding increased  $\lambda_{\parallel}$  and  $\lambda_{\perp}$  we observed in the external/extreme capsule and corpus callosum indicates severe tract damage related to advanced stages of wallerian degeneration,<sup>18</sup> possibly as a result of cortical and subcortical GM pathology. This pattern is at variance with that observed in earlier stages of wallerian degeneration and in demyelination, in which decreased FA is accompanied by a decrease or nonsignificant change of  $\lambda_{\parallel}$ , whereas  $\lambda_{\perp}$  is increased.<sup>14,35</sup>

In our series, TBSS also showed increased FA in the supralenticular corticospinal tracts and frontal WM, which was associated with increased  $\lambda_{\parallel}$  in the absence of any significant change of  $\lambda_{\perp}$ . Significantly increased FA was documented by using the region-of-interest and voxelwise analyses of Rosas et al<sup>12</sup> in the anterior limbs and genu of the internal capsule in presymptomatic and early symptomatic HD, but they did not comment on this “unexpected” finding. To our knowledge, the mechanisms underlying increased FA are not established. Because FA depends on orientation, diameter and packing of the WM fibers, degree of myelination,<sup>36</sup> and axonal flux, FA increase might be due to selective damage of fibers running

orthogonal to the fibers showing increased FA, resulting in an overall “apparent” increase of the anisotropy at the voxel level, or due to a peculiar type or severity of tract degeneration. The lack of clinical correlates of the areas of increased FA in our patients seems to confirm the first hypothesis. Further investigations are, however, needed to clarify this issue.

As opposed to the spatially selective decrease (or increase) of the FA, we observed extensive clusters of increased MD, with or without significant changes in the corresponding FA maps, which involved multiple association tracts, including the arciform fibers of the cerebral hemispheres, the corpus callosum, and the midbrain WM. However, no WM damage was observed in the cerebellum, pons, and medulla. This is in line with the view that HD is characterized by a distributed pattern of white matter changes.<sup>12,13</sup>

While most studies focused on the correlation between the subcortical and cortical GM atrophy and the genetic and clinical features,<sup>19,22</sup> Jech et al<sup>37</sup> also found a correlation between WM volume loss and both the number of abnormal triplets and the UHDRS motor score. In line with prior VBM investigations,<sup>37,38</sup> in our study parametric VBM analysis demonstrated significant correlation of the motor and executive function deficits with atrophy of the neostriatum and the cerebral cortex. The same deficits also correlated with multiple areas of WM atrophy, including the internal capsule, corpus callosum, and cerebellum, thus confirming and extending previous findings that were limited to the motor impairment.<sup>37</sup>

More interestingly, we observed a correlation between microstructural damage of the residual WM, in terms of decreased FA or increased MD, with the clinical features, including motor and cognitive performances, confirming prior observations.<sup>10,12,13</sup> In particular, the microstructural damage of several WM tracts within and beyond the corpus callosum showed a correlation with cognitive deficits.<sup>12</sup> In consideration of the relative preservation of the limbic prefrontal cortex in HD<sup>32</sup> and the presumed capability of the Stroop test to explore the frontal functions,<sup>39</sup> the correlation between the frontal WM atrophy and microstructural change and the Stroop test observed in our study seems to confirm the hypothesis of Klöppel et al<sup>13</sup> that selective WM damage might explain some symptoms and signs in HD, independent of cortical GM damage. We observed more widespread correlation between clinical variables and MD than between clinical variables and FA and a unique correlation of MD with disease duration. These 2 features would support the use of MD in addition to FA as a surrogate marker of disease progression, also in view of a hypothetic restoration of WM microstructural integrity to be pursued by new therapies of HD. Although so far such a potential of DTI is unproved in the case of neurodegenerative diseases, increase of FA in a middle cerebellar peduncle lesion following highly active antiretroviral therapy was documented in a patient with progressive multifocal leukoencephalopathy.<sup>40</sup>

## Conclusions

Overall, the present results confirm that substantial damage of the WM, in terms of loss of bulk and microstructural changes of the remaining WM, is part of the neurodegenerative process of HD and could explain the varying and complex symptoms of the disease. However, the relationship between GM and

WM changes as well as between WM atrophy and microstructural damage remains to be established. In particular, the possibility that WM damage in HD could reflect ongoing damage of the glial cells or abnormalities in axonal transport rather than simply representing wallerian degeneration or a dying-back phenomenon secondary to GM pathology should be explored in future studies. MR imaging-based measures could be considered as a biomarker of neurodegeneration in HD gene carriers.

## References

1. A novel gene containing a trinucleotide repeat that is expanded and unstable on Huntington's disease chromosome: The Huntington's Disease Collaborative Research Group. *Cell* 1993;72:971–83
2. de la Monte SM, Vonsattel JP, Richardson EP Jr. Morphometric demonstration of atrophic changes in the cerebral cortex, white matter, and neostriatum in Huntington's disease. *J Neuropathol Exp Neurol* 1988;47:516–25
3. Thieben MJ, Duggins AJ, Good CD, et al. The distribution of structural neuropathology in pre-clinical Huntington's disease. *Brain* 2002;125:1815–28
4. Beglinger LJ, Nopoulos PC, Jorge RE, et al. White matter volume and cognitive dysfunction in early Huntington's disease. *Cogn Behav Neurol* 2005;18:102–07
5. Ciarmiello A, Cannella M, Lastoria S, et al. Brain white-matter volume loss and glucose hypometabolism precede the clinical symptoms of Huntington's disease. *J Nucl Med* 2006;47:215–22
6. Tabrizi SJ, Langbehn DR, Leavitt BR, et al. Biological and clinical manifestations of Huntington's disease in the longitudinal TRACK-HD study: cross-sectional analysis of the baseline data. *Lancet Neurol* 2009;8:791–801
7. Aylward EH, Anderson NB, Bylsma FW, et al. Frontal lobe volume in patients with Huntington's disease. *Neurology* 1998;50:252–58
8. Fennema-Notestine C, Archibald SL, Jacobson MW, et al. In vivo evidence of cerebellar atrophy and cerebral white matter loss in Huntington disease. *Neurology* 2004;63:989–95
9. Gavazzi C, Della Nave R, Petralli R, et al. Combining functional and structural MR imaging of the brain in Huntington disease. *J Comput Assist Tomogr* 2007;31:574–80
10. Mascalchi M, Lolli F, Della Nave R, et al. Volumetric, diffusion and magnetization transfer MR imaging of the brain in individuals with Huntington's disease. *Radiology* 2004;232:867–73
11. Reading SA, Yassa MA, Bakker A, et al. Regional white matter changes in pre-symptomatic Huntington's disease. *J Psychiat Res* 2005;140:55–62
12. Rosas HD, Tuch DS, Hevelone ND, et al. Diffusion tensor imaging in presymptomatic and early Huntington's disease: selective white matter pathology and its relationship to clinical measures. *Mov Disord* 2006;21:1317–25
13. Klöppel S, Draganski B, Golding CV, et al. White matter connections reflect changes in voluntary-guided saccades in pre-symptomatic Huntington's disease. *Brain* 2008;131:196–204
14. Weaver KE, Richards TL, Liang O, et al. Longitudinal diffusion tensor imaging in Huntington's disease. *Exp Neurol* 2009;216:525–29
15. Smith SM, Jenkinson M, Johansen-Berg H, et al. Tract-based spatial statistics: voxelwise analysis of multi-subject diffusion data. *Neuroimage* 2006;31:1487–505
16. Smith SM, Johansen-Berg H, Jenkinson M, et al. Acquisition and voxelwise analysis of multi-subject diffusion data with tract-based spatial statistics. *Nat Protoc* 2007;3:499–503
17. Della Nave R, Ginestroni A, Tessa C, et al. Brain white matter tracts degeneration in Friedreich ataxia: an in vivo MRI study using tract-based spatial statistics and voxel based morphometry. *Neuroimage* 2008;40:19–25
18. Della Nave R, Ginestroni A, Tessa C, et al. Brain white matter damage in SCA1 and SCA2: an in vivo study using voxel-based morphometry, histogram analysis of mean diffusivity and tract-based spatial statistics. *Neuroimage* 2008;43:10–19
19. Muglia M, Leone O, Annesi G, et al. Nonisotopic method for accurate detection of (CAG)<sub>n</sub> repeats causing Huntington disease. *Clin Chem* 1996;42:1601–03
20. Rubinsztein DC, Leggo J, Coles R, et al. Phenotypic characterization of individuals with 30–40 CAG repeats in the Huntington disease (HD) gene reveals HD cases with 36 repeats and apparently normal elderly individuals with 36–39 repeats. *Am J Hum Genet* 1996;59:16–22
21. Unified Huntington's Disease Rating Scale: reliability and consistency—Huntington Study Group. *Mov Disord* 1996;11:136–42
22. Rosas HD, Salat DH, Lee SY, et al. Cerebral cortex and the clinical expression of Huntington's disease: complexity and heterogeneity. *Brain* 2008;131:1057–68
23. Treisman A, Fearnley S. The Stroop test: selective attention to colours and words. *Nature* 1969;222:437–39
24. Wechsler D. *Manual for the Wechsler Adult Intelligence Scale-Revised*. New York: The Psychological Corp; 1981

25. Shoulson I, Fahn S. **Huntington disease: clinical care and evaluation.** *Neurology* 1979;29:1–3
26. Behrens TE, Woolrich MW, Jenkinson M, et al. **Characterization and propagation of uncertainty in diffusion-weighted MR imaging.** *Magn Reson Med* 2003;50:1077–88
27. Smith SM, Jenkinson M, Woolrich MW, et al. **Advances in functional and structural MR image analysis and implementation as FSL.** *Neuroimage* 2004;23:208–19
28. Good CD, Johnsrude IS, Ashburner J, et al. **A voxel-based morphometric study of ageing in 465 normal adult human brains.** *Neuroimage* 2001;14:21–36
29. Nichols TE, Holmes AP. **Nonparametric permutation tests for functional neuroimaging: a primer with examples.** *Hum Brain Mapp* 2002;15:1–25
30. Mori S, Wakana S, van Zijl PC, et al. *MRI Atlas of Human White Matter.* Amsterdam, the Netherlands: Elsevier; 2005
31. Kassubek J, Juengling FD, Kioschies T, et al. **Topography of cerebral atrophy in early Huntington's disease: a voxel-based morphometric MRI study.** *J Neurol Neurosurg Psychiatry* 2004;75:213–20
32. Muhlau M, Weindl A, Wolschlag AM, et al. **Voxel-based morphometry indicates relative preservation of the limbic prefrontal cortex in early Huntington disease.** *J Neural Transm* 2007;114:367–72
33. Budde MD, Kim JH, Liang HF, et al. **Toward accurate diagnosis of white matter pathology using diffusion tensor imaging.** *Magn Reson Med* 2007;57:688–95
34. Schmahmann JD, Pandya DN. *Fibre Pathways of the Brain.* New York: Oxford University Press; 2006
35. Cosottini M, Giannelli M, Siciliano G, et al. **Diffusion-tensor MR imaging of corticospinal tract in amyotrophic lateral sclerosis and progressive muscular atrophy.** *Radiology* 2005;237:258–64
36. Pierpaoli C, Barnett A, Pajevic S, et al. **Water diffusion changes in wallerian degeneration and their dependence on white matter architecture.** *Neuroimage* 2001;13:1174–85
37. Jech R, Klempff J, Vymazal J, et al. **Variation of selective gray and white matter atrophy in Huntington's disease.** *Mov Disord* 2007;22:1783–89
38. Peinemann A, Schuller S, Pohl C, et al. **Executive dysfunction in early stages of Huntington's disease is associated with striatal and insular atrophy: a neuro-psychological and voxel-based morphometric study.** *J Neurol Sci* 2005;239:11–19
39. Goldberg E, Bougakov D. **Neuropsychological assessment of frontal lobe dysfunction.** *Psychiatr Clin North Am* 2005;28:567–80
40. Usiskin SI, Bainbridge A, Miller RF, et al. **Progressive multifocal leuko-encephalopathy: serial high b-value diffusion-weighted MR imaging and apparent diffusion coefficient measurements to assess response to highly active antiretroviral therapy.** *AJNR Am J Neuroradiol* 2007;28:285–86